1016 *Macromolecules* **2011**, *44*, 1016–1025
DOI: 10.1021/ma102503j

Macromolecules
ARTICLE

Effect of Concentration on the Glass Transition and Viscoelastic Properties of Poly(methyl methacrylate)/Ionic Liquid Solutions

Michelle M. Mok,[†] Xingcheng Liu,[†] Zhifeng Bai,[†] Yu Lei,[†] and Timothy P. Lodge*[,†,‡]

[†]*Department of Chemistry and* [‡]*Department of Chemical Engineering & Materials Science, University of Minnesota, Minneapolis, Minnesota 55455, United States*

Received November 3, 2010; Revised Manuscript Received December 31, 2010

ABSTRACT: The glass transition behavior and viscoelastic properties of poly(methyl methacrylate) in mixtures with the ionic liquid 1-ethyl-3-methylimidazolium bis(trifluoromethylsulfonyl)imide are examined at compositions from 10 wt % polymer to pure polymer, over the temperature range from −180 to 230 °C. Polymers of two different molecular weights (125 and 335 kg/mol) are studied. Glass transitions are analyzed by differential scanning calorimetry, and derivative heat flow curves are used to extract glass transition temperatures and breadths. Distinct composition dependences are observed for the polymer and ionic liquid components, with two apparent glass transitions at intermediate compositions. The glass transition breadths of the mixtures (∼30−70 °C) are much broader than those of the pure components (< 25 °C). These results reflect distinct effective local compositions arising from the chain connectivity of the polymer component. The frequency-dependent dynamic moduli G' and G'' show a shift from unentangled to entangled behavior as concentration is increased from 10 to 20 wt % polymer. The application of time−temperature superposition is successful over the full range of compositions, leading to master curves extending up to 11 orders of magnitude in reduced frequency. The plateau modulus (G_N) exhibits a concentration dependence of $G_N \sim c^{2.2}$, and analyses of the longest relaxation times and viscosity show the general trends expected for entangled solutions of increasing polymer concentration. Overall, ionic liquids are demonstrated to be effective model solvents for studying viscoelastic properties over wide temperature and composition ranges due to their nonvolatility and stability.

Introduction

Ionic liquids are highly versatile solvents that have been increasingly used for their unique properties of extremely low vapor pressure, thermal and chemical stability, tunable solvation, nonflammability, and ionic conductivity. With respect to polymers, ionic liquids were first developed as solvents for polymerization, but now more investigations have focused on incorporating them within polymer systems for their materials properties.[1−3] Polymer/ionic liquid combinations have shown potential for applications over a wide range of compositions. For example, at the concentrated end of the spectrum, ionic liquids have been studied as plasticizers,[4−10] demonstrating mechanical enhancements comparable to traditional phthalate plasticizers, but with superior high-temperature stability,[4−6,8] reduced leaching,[7,9] and enhanced solubility.[4−6,10] Intermediate to semidilute compositions,[11−19] including phase-separated systems based on block copolymers,[20−33] have been studied as rubbery to gel-like matrices. Applications include fuel cell and separations membranes,[12,24] dielectric layers in plastic electronics,[29−32] and gel electrolytes for batteries.[11,13−18,28] In these systems the ionic liquids are used for their specific functionality (e.g., high ionic conductivity), while the polymeric component imparts mechanical and structural properties. Finally, at the most dilute level, homopolymers in ionic liquids have been proposed as designer solvents,[34] while block copolymers in ionic liquids have been studied for their micelle- and vesicle-forming capabilities[35−40] with potential applications as vessels for transport and extraction within biphasic systems.[41,42]

*Author for correspondence. E-mail: lodge@umn.edu.

Despite the interest in polymer−ionic liquid systems, there are few reports on basic properties spanning from the dilute regime to the concentrated regime. For example, some glass transition studies have been carried out at higher polymer concentrations, in investigations of ionic liquids as plasticizers[4−10] and as selective solvents within phase-separated block copolymers.[24−26,28,33] A more extended range of compositions was studied for a cross-linked polymer−ionic liquid material,[15,16] but without reference to glass transition breadths. No systematic studies of polymer−ionic liquid viscoelastic properties as a function of composition have been reported. Thus, there is a need for a comprehensive study of glass transition and viscoelastic behaviors in polymer−ionic liquid systems over the full composition range. These trends dictate the mechanical properties of the materials, determining their range of usable temperatures as well as their potential processability. Other properties of interest, such as ionic conductivity or permeability, may also be correlated directly to rheological features. Finally, it is of interest to compare these results to those obtained for polymers in conventional solvents to ascertain whether any features unique to the ionic nature of the solvent arise. Ionic liquids are intrinsically complex solvents, capable of different simultaneous solvent−solute interaction behavior.[43] In conductivity studies, for example, stronger interactions have been reported in one system between the anion species of the ionic liquid and polymer matrix than the cation species.[2] Also, T_gs higher than the neat copolymer components have been reported for block copolymer/ionic liquid systems;[24,28] this has been related to the effect of salt ions acting to form physical cross-links in polymer electrolyte systems.[24]

 Published on Web 01/19/2011

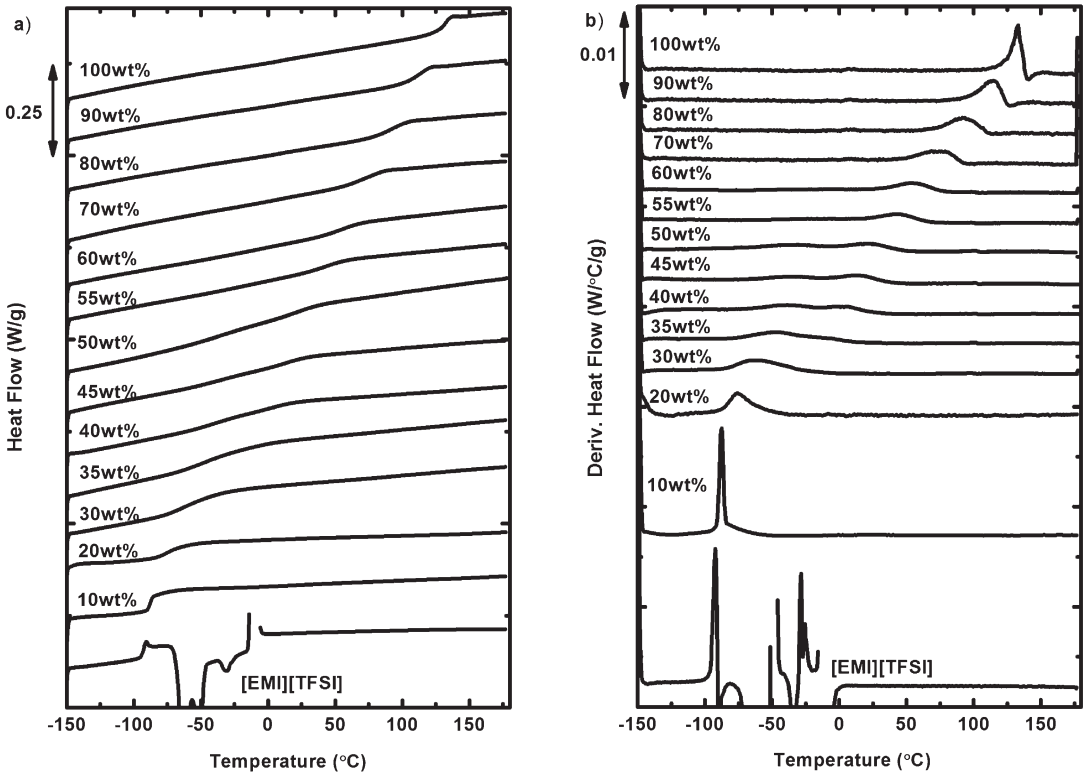

Figure 1. DSC (a) heat flow and (b) derivative heat flow curves for 125K PMMA prepared at different weight fractions in [EMI][TFSI].

Traditionally, calorimetric studies of polymers and solvents were expected to yield single glass transitions that varied monotonically with composition change, following trends similar to those described by additivity rules such as the Fox equation[44] or the Gordon−Taylor equation.[45] Recent detailed studies[46−59] have revealed the potential for more complex behavior: dual, broadened glass transitions[50,51,53−55] with separate composition dependences.[46−56,59] These results have been explained using the Lodge−McLeish model[54,60−62] through the increased effective local concentrations of polymer or solvent due to self-concentration effects arising from the chain connectivity of the monomer units.[54−56,58,59] Meanwhile, extensive rheological studies of polymer solutions have been carried out to determine their structural and viscoelastic properties as a function of concentration.[63−71] The results in the terminal, plateau, and initial part of the transition zone have largely been explained by predictions based on the Zimm, Rouse, and reptation models for the dilute, semidilute, and concentrated regimes, respectively.[72−74] While these studies have emphasized the effects of a diluent on polymer chain dynamics, fundamental studies based on polychlorinated biphenyls (Aroclors)[75−77] and other solvent systems[47,59] have also shown that polymer chains can have an effect on small-molecule dynamics.

The focus of this study is to examine the behavior of poly(methyl methacrylate) (PMMA) of two molecular weights in 1-ethyl-3-methylimidazolium bis(trifluoromethylsulfonyl)imide ([EMI][TFSI]) over the range of compositions from dilute polymer to pure polymer using differential scanning calorimetry and rheometry. We choose this as a model polymer−ionic liquid system since PMMA and [EMI][TFSI] are known to be compatible over this full range of compositions.[15,16,78,79] Also, the component glass transition temperatures are extremely widely separated, yielding a large temperature window for the glass transition studies. Finally, both PMMA and [EMI][TFSI] are already commonly studied in the field of polymer−ionic liquid materials, both in conjunction with each other[15,16,30,32,33,36,38,78] and within other polymer−ionic liquid pairs.[5,10,17,21−23,28,37,39−41]

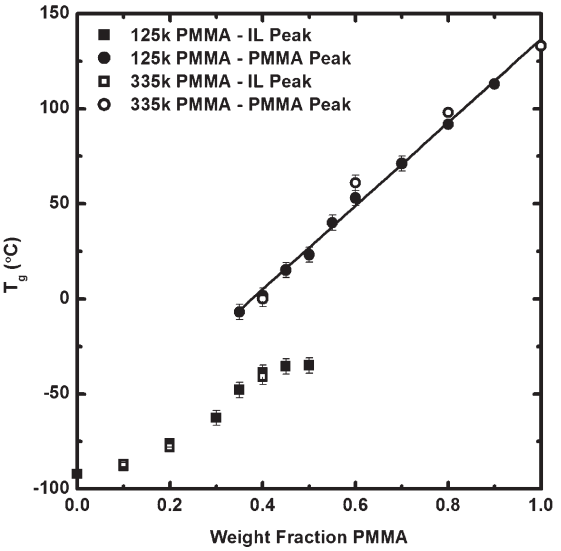

Figure 2. Variation of T_g with weight fraction of polymer in [EMI][TFSI] for 125K and 335K PMMA. Values were extracted from the peak positions in the DSC derivative heat flow curves. The solid line is a linear fit of the PMMA peak T_g values.

Experimental Section

Materials and Blends. The PMMA polymers were previously synthesized by Zeroni[80] using anionic polymerization. The number-average molecular weights of the polymers are 125 kg/mol ($M_w/M_n = 1.02$) and 335 kg/mol ($M_w/M_n = 1.21$), as characterized by size exclusion chromatography. The ionic liquid [EMI][TFSI] was synthesized using a method described previously.[15] The product was dried in a vacuum oven at ~60 °C for 3 days.

The PMMA/ionic liquid solutions were prepared by combining the polymer and ionic liquid at appropriate weight ratios and

Table 1. Glass Transition Temperatures and Transition Widths for 125K PMMA

	[EMI][TFSI] (°C)				PMMA (°C)			
PMMA wt fraction	T_g (±2 °C)	onset (±5 °C)	end (±5 °C)	ΔT_g	T_g (±2 °C)	onset (±5 °C)	end (±5 °C)	ΔT_g
0	−92	−96	−90	6				
0.10	−88	−91	−57	34				
0.20	−76	−86	−38	48				
0.30	−63	−83	−17	66				
0.35	−48	−80	−13	67	−7	−13	18	31
0.40	−39	−73	−15	58	2	−15	29	44
0.45	−36	−72	−11	61	15	−11	43	54
0.50	−35	−68	−6	62	23	−6	50	56
0.55		−59	12	71	40	12	68	56
0.60		−57	19	76	53	19	79	60
0.70					71	48	93	45
0.80					92	69	111	42
0.90					113	90	126	36
1.00					133	123	139	16

Table 2. Glass Transition Temperatures and Transition Widths for 335K PMMA

	[EMI][TFSI] (°C)				PMMA (°C)			
PMMA wt fraction	T_g (±2 °C)	onset (±5 °C)	end (±5 °C)	ΔT_g	T_g (±2 °C)	onset (±5 °C)	end (±5 °C)	ΔT_g
0	−92	−96	−90	6				
0.10	−87	−90	−60	30				
0.20	−78	−89	−47	42				
0.40	−41	−82	−16	66	0	−16	21	37
0.60		−55	47	102	61	47	79	32
0.80					98	82	109	27
1.00					133	116	140	24

adding excess methylene chloride as a cosolvent to facilitate dissolution. These solutions were stirred until homogeneous. The cosolvent was then removed by a gentle nitrogen purge at room temperature for >12 h, followed by heating in a vacuum oven (~30 mTorr) at elevated temperatures for >24 h or until a constant weight was achieved. The blends of lower PMMA concentration were held at temperatures >70 °C, while the blends of highest PMMA concentration were heated at temperatures exceeding the glass transition temperature of the pure polymer (~130 °C). All samples appeared transparent and homogeneous by eye. Samples were stored in a vacuum desiccator.

Differential Scanning Calorimetry (DSC). Measurements were taken on a TA Instruments Q1000 DSC instrument with liquid nitrogen cooling capabilities. Samples (~4−10 mg) were sealed within either aluminum hermetic pans or regular aluminum pans provided by TA Instruments and measured against an equivalent empty pan as reference. Helium was used as the purge gas. The samples were heated to 180 °C (10 °C/min) and equilibrated before being cooled at a rate of either 30 or 10 °C/min to −150 °C. Measurements were then obtained during a heating ramp from −150 to 180 °C at 10 °C/min. No difference in glass transition was found between heating scans from samples cooled using the 30 and 10 °C/min cooling rates, and results from the 10 °C/min cooling rate measurements are reported. Repeated heating scan measurements from both cooling rates were also found to be equivalent.

Rheology. Linear viscoelastic measurements were obtained on a TA Instruments ARES rheometer using low-amplitude oscillatory shear. The instrument was equipped with a convection oven with nitrogen and liquid nitrogen cooling capabilities. Measurements were taken using 8, 25, or 50 mm diameter parallel plates as appropriate for the different concentrations, and the sample gap was ~1 mm. Samples with lower PMMA weight fraction were loaded directly, while those with >60 wt % PMMA were first hot-pressed using molds into appropriately sized disks at 200 °C for loading. Care was taken to exclude bubbles. Samples were subjected to strain sweeps to verify their linear region of strain response, and then frequency sweeps were taken using shear strains of 10% or less. Measurements were taken at decreasing temperatures.

Results and Discussion

DSC Results. The DSC results for the 125K PMMA solutions are shown in Figure 1, while the results for the 335K PMMA solutions can be found in the Supporting Information (Figure S1). In both cases, the heat flow data and the derivative of the heat flow data are provided. The derivatives were taken using an interval of 1 °C. The step functions in DSC heat flow curves traditionally associated with the occurrence of glass transitions are rendered as peaks in the derivative plots, and transition breadths can be more easily extracted.[61,62,81]

The curves for pure [EMI][TFSI] show a sharp glass transition at ~−90 °C followed by crystallization and melting events between −75 and 0 °C (these signals have been truncated since our focus is on the glass transition). This is consistent with previous DSC results for the pure ionic liquid.[15,16,33] The curves for pure PMMA exhibit only a single glass transition at ~130 °C; while broader than the [EMI][TFSI] glass transition, the breadth is typical of that for homopolymers.[81] Both the pure [EMI][TFSI] and PMMA glass transitions show an enthalpy overshoot.

With the addition of 10 wt % PMMA, all signatures of solvent crystallization and melting are no longer present, for both the 125K and 335K PMMA. This indicates that the rate of crystallization at 10 wt % polymer is slower than the rates of heating and cooling used in the measurements.[55] The glass transition signature remains narrow, although it is shifted very slightly to higher temperatures and the enthalpy overshoot is gone. A broadened tail can be observed in the derivative curve toward higher temperatures, and this broadening is more prominent in the 10 wt % 335K PMMA sample.

With increasing weight fraction to 20 wt %, the glass transition loses its sharpness and continues a shift to higher

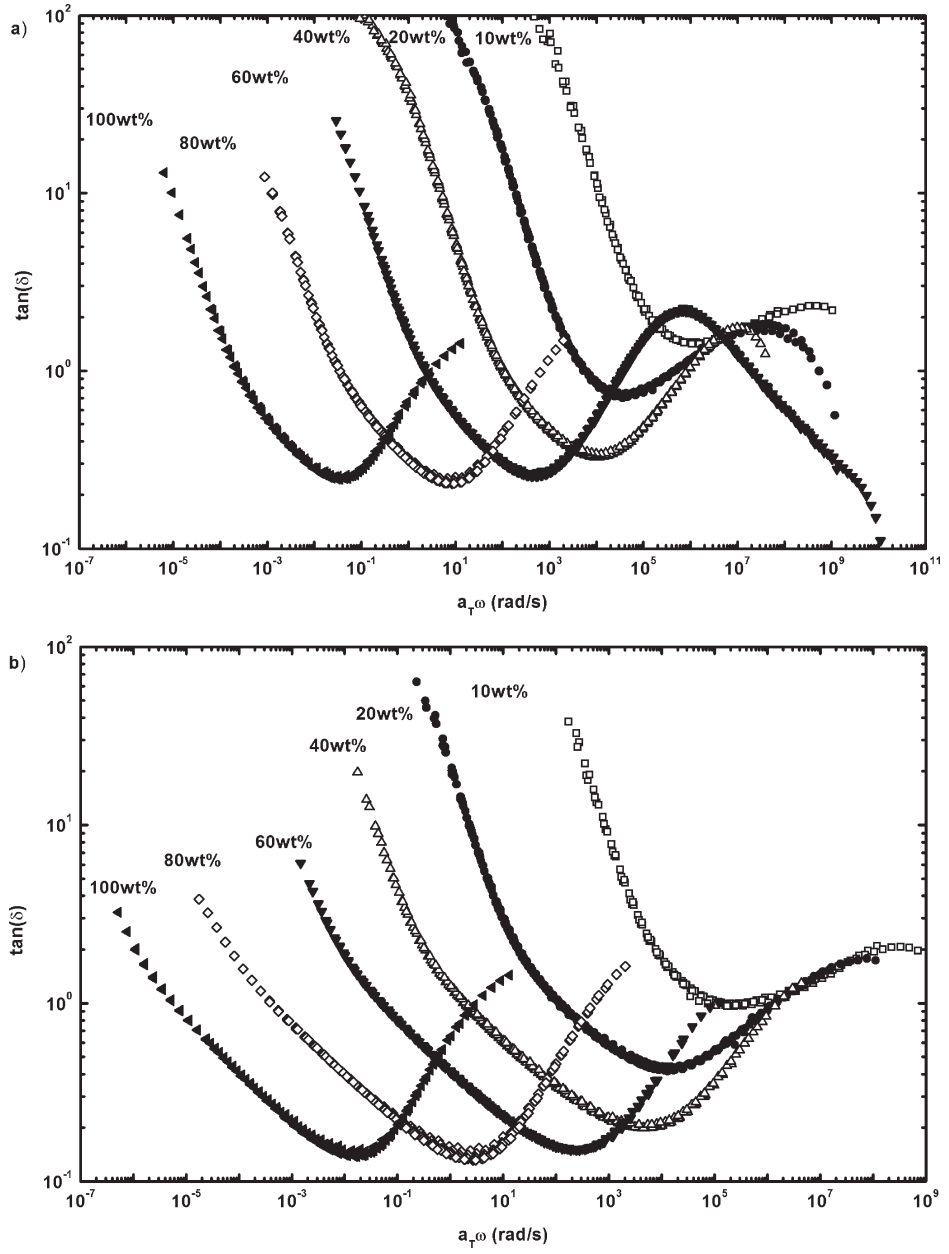

Figure 3. tTS master curves of tan(δ) with T_{ref} = 150 °C for (a) 125K and (b) 335K PMMA prepared at different weight fractions in [EMI][TFSI].

temperatures; the presence of a tail toward higher temperatures can still be seen. At 30 wt %, the transition broadens to the point where the derivative curve appears multimodal. For blends between 35 and 50 wt %, the step change in the heat flow curves is substantially broadened, and the derivative heat flow curves take on a bimodal appearance, suggesting responses from regions richer in either [EMI][TFSI] or PMMA. Consistent with this, there is also a shift in signal intensity from the lower temperature peak to the higher temperature peak with increasing PMMA content. Both peaks also continue to shift to higher temperatures with additional PMMA.

Between 55 and 60 wt % PMMA, the heat flow response appears as one main peak associated with PMMA-rich regions, while the signature of the [EMI][TFSI]-rich regions has diminished to the point where it is no longer a clear peak, but more an extended transition. Finally, from 70 to 100 wt % PMMA, this region disappears, and only a single glass transition region remains, which progressively narrows and shifts to higher temperatures with increasing PMMA content. The enthalpy overshoot reappears between 80 and 90 wt %. Very similar DSC heat flow results were observed by Watanabe and co-workers[15,16] in their studies of PMMA polymerized at different concentrations in [EMI][TFSI] with cross-linkers. While noticeably broadened glass transitions were also obtained at intermediate compositions, these were interpreted as single transitions.

Discussion of DSC Results. The trends described above are quantified by extraction of glass transition temperatures (T_gs) and glass transition temperature breadths (ΔT_gs). The T_g values were determined from the peak maxima of the derivative heat flow curves and are plotted as a function of PMMA weight fraction in Figure 2 and listed in Tables 1 and 2. Associated ΔT_g values were determined from the onsets and ends of deviation from the derivative heat flow curve baselines and are listed in Tables 1 and 2.

The data corresponding to higher and lower PMMA compositions that exhibited single T_g peaks form distinct

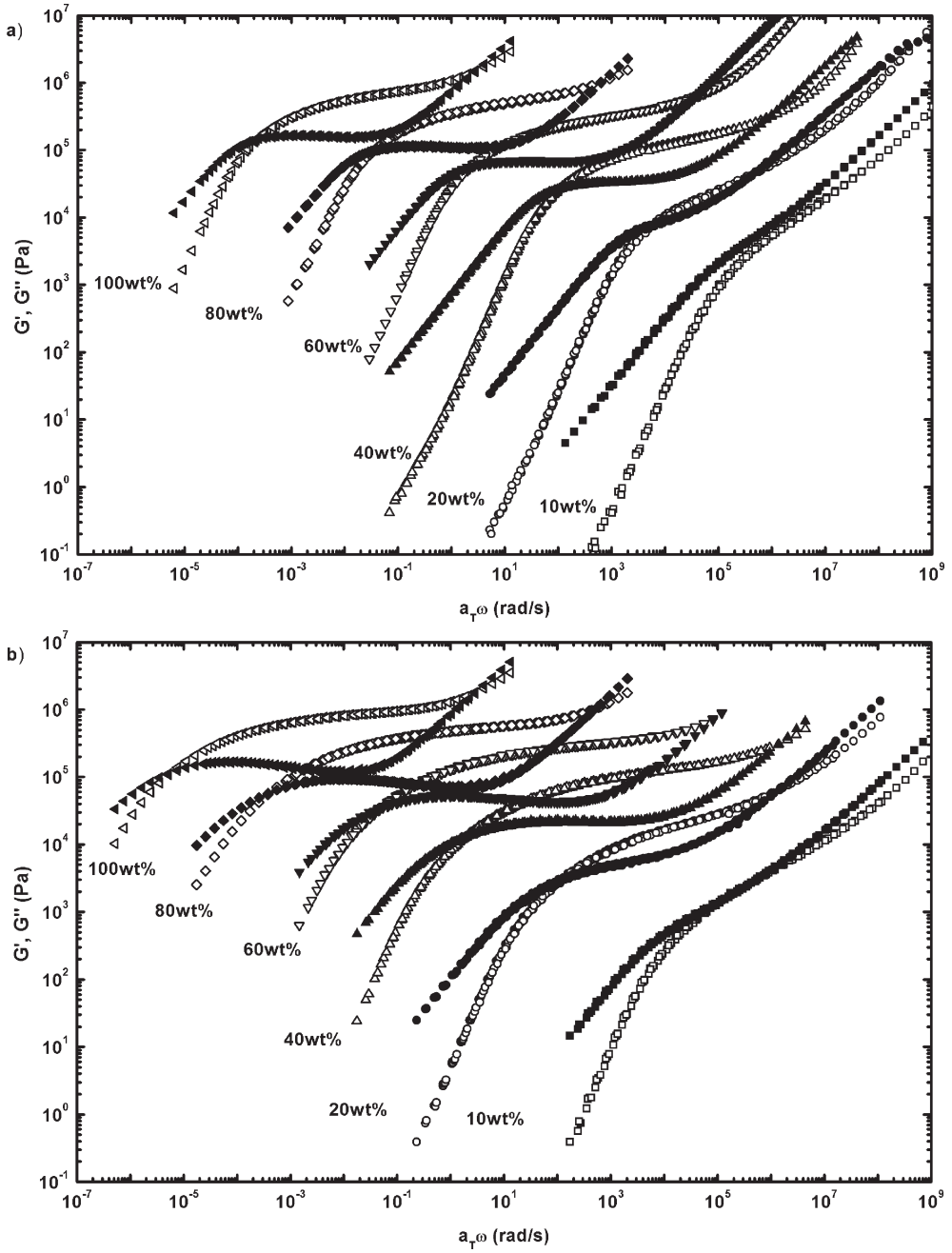

Figure 4. tTS master curves of dynamic shear moduli (G' (open symbols) and G'' (closed symbols)) with T_{ref} = 150 °C for (a) 125K and (b) 335K PMMA prepared at different weight fractions in [EMI][TFSI].

sets of composition-dependent T_g behavior in Figure 2. The two T_gs corresponding to samples with dual peaks continue to trace these distinct composition dependences to intermediate compositions. The data associated with the ionic liquid-rich peaks are at lower temperatures and PMMA compositions, while the data associated with PMMA-rich peaks are at higher temperatures and PMMA compositions. The results for 125K and 335K PMMA are the same within error, as expected for polymers of such high molecular weight. The composition dependence of the PMMA-rich peak T_gs can be fit to a straight line (T_g [°C] = $219w_{PMMA} - 83$, where w_{PMMA} is the weight fraction of PMMA) and is stronger in composition dependence than the ionic liquid-rich peak T_gs.

The appearance of two distinct composition dependences[46−56,59] and two glass transitions[50,51,53−55] is consistent with previous studies of polymer−solvent systems by dilatometry,[46] DSC,[46−55] NMR,[56] and dielectric relaxation spectroscopy (DRS).[47,55,59] This phenomenon has been explained by Savin et al.[54] with reference to the Lodge−McLeish model,[60−62] which had been developed to account for the appearance of two glass transitions in miscible A/B polymer blends. The two transitions are attributed to the existence of A-rich and B-rich effective local concentrations that arise by virtue of chain connectivity and are at length scales of relevance to T_g dynamics. The weaker composition dependence of the lower T_g component is explained by the potential for higher self-concentrations in the more flexible molecule, yielding behavior closer to that of the pure component. Savin et al.[54] suggested that similar effects could take place in polymer/solvent blends, despite there being chain connectivity for only one of the components. Subsequent studies have supported this.[55,56,58,59]

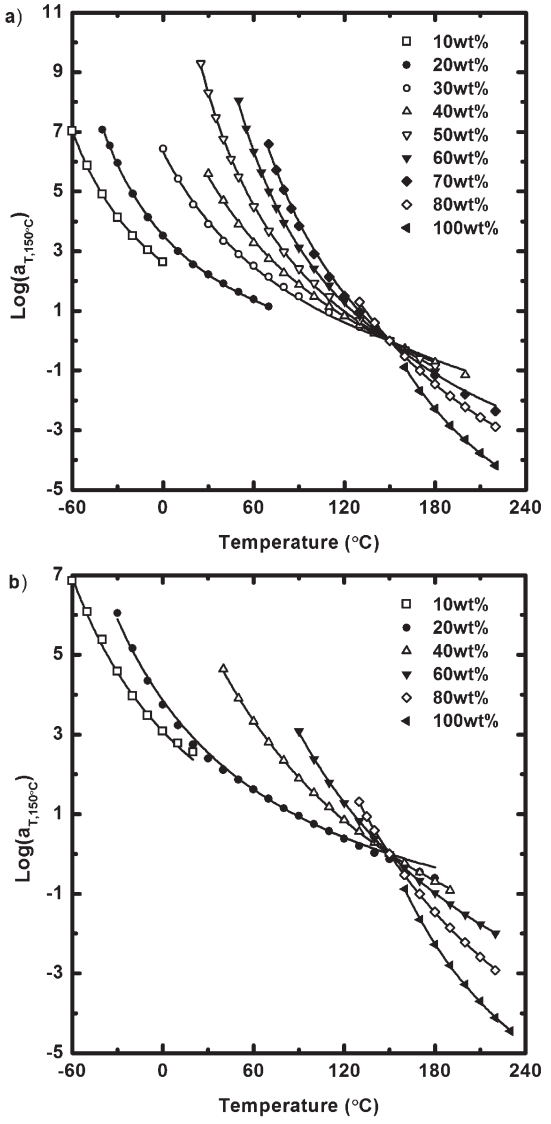

Figure 5. Shift factors from tTS master curves as a function of temperature with T_{ref} = 150 °C for (a) 125K and (b) 335K PMMA prepared at different weight fractions in [EMI][TFSI]. Solid lines indicate WLF fits.

Focusing on ΔT_gs, it can be seen that the transitions are substantially broader in all solution cases than those of the pure components. Such broadening is consistent with past observations for other polymer−solvent blends as measured by DSC[49,50,54,55] and DRS.[47,55] While the Lodge−McLeish model does not quantitatively account for distributions in compositions, it can be used to explain them qualitatively based on ranges of effective local concentration induced by chain connectivity and self-concentrations. A model used by Kumar, Colby, and co-workers[82,83] to combine effects from self-concentration and concentration fluctuations has been found to be a good predictor of segmental relaxation time distributions; the length scale of importance was found to correlate to that postulated in the Lodge−McLeish model. The concept of self-concentrations could also explain the broadened tail seen in the 10 and 20 wt % PMMA cases. The tail region may represent the [EMI][TFSI] molecules that are in greater contact with PMMA segments, while those ionic liquid molecules associated with the sharp peak are primarily in contact with other ionic liquid molecules. Similar explanations have previously been given for the broadened DSC ΔT_gs in solutions of low polymer concentration[55] and also in DRS measurements for the broadened α-processes of solvent molecules in polymer solutions.[47,59]

Overall, the glass transition behavior observed for the PMMA/[EMI][TFSI] system closely resembles that of mixtures of polymers with conventional solvents. The increase in T_g reported in certain block copolymer/ionic liquid systems[24,28] may arise from interactions specific to those polymer/ionic liquid combinations in combination with self-assembly effects.

Rheology Results. Master curves of tan(δ) as a function of reduced frequency using time−temperature superposition (tTS) with a reference temperature of 150 °C are compiled in Figure 3 for selected PMMA compositions (plots for the remaining compositions can be found in Supporting Information Figure S2). The same frequency shifts were applied to the G' and G'' data to create the tTS master curves shown in Figure 4 (plots for remaining compositions can be found in Supporting Information Figure S3). Small vertical shifts have also been applied to the G' and G'' data.

At 10 wt % PMMA, both the 125K and 335K PMMA master curves show unentangled behavior, with the minimum of tan(δ) equal to or exceeding a value of 1, and no crossover or plateau region is evident in the G' and G'' evolution from glassy behavior to terminal behavior. The behavior of the 10 wt % 125K case resembles that of dilute solutions,[72] with G' and G'' completely separated. Meanwhile, the 10 wt % 335K case more closely resembles that of semidilute, unentangled solutions,[72] with G' and G'' almost equal over the glassy to terminal transition region.

With an increase to 20 wt % PMMA, evidence of entangled behavior[72−74] appears as a plateau begins to emerge in both the 125K and 335K PMMA cases; the tan(δ) minimum decreases below a value of 1, and two crossovers appear as G' exceeds G'' in the region between glassy and terminal behavior. With increasing PMMA content to 60 wt %, this region increases to span 4 decades of time in the 125K PMMA blends and 6 decades in the 335K PMMA blends; concurrently, the minimum in tan(δ) decreases as the separation between G' and G'' in this zone grows. Over the whole concentration range, the crossover from rubbery to terminal behavior shifts to lower frequencies by 2−3 decades for every 20 wt % increase in PMMA content, while the moduli in the plateau region shift to higher values with increasing PMMA. Finally, the crossover from glassy to rubbery behavior also shifts to lower frequencies by 2−3 decades at higher PMMA concentrations, but for PMMA compositions $<$40 wt %, there is a much smaller shift. This supports the trend found by DSC, of T_gs depending more highly on composition at higher concentrations compared to lower concentrations. Some of the higher concentration curves show subtle deviations from perfect tTS in tan(δ) and G'' in the plateau region; this has been observed in other systems and is ascribed to the different temperature dependences of relaxation modes associated with very short length scales at the high frequencies at which the preshifted measurements were taken.[84,85]

The shift factors (a_T) which were used in the tTS process are shown in Figure 5, relative to a reference temperature of 150 °C using the Williams−Landel−Ferry (WLF) equation:[74]

$$\log a_T = -\frac{C_1(T - T_{ref})}{C_2 + (T - T_{ref})} \quad (1)$$

where T_{ref} is the reference temperature and C_1 and C_2 are fitting parameters. An increase in the steepness of a_T near the reference temperature is seen with increasing

Table 3. WLF Fitting Parameters and Vogel Temperatures with T_{ref} = 150 °C

	125K PMMA			335K PMMA		
PMMA wt fraction	C_1	C_2 (°C)	T_0 (°C)	C_1	C_2 (°C)	T_0 (°C)
0.10	2.2	275	−125	3.4	314	−164
0.20	2.5	258	−108	3.2	277	−127
0.30	4.7	262	−112			
0.40	5.9	248	−98	6.8	273	−123
0.50	5.6	201	−51			
0.60	6.1	176	−26	8.4	224	−74
0.70	7.6	175	−25			
0.80	10.3	181	−31	10.5	184	−34
1.00	10.7	111	39	10.5	109	41

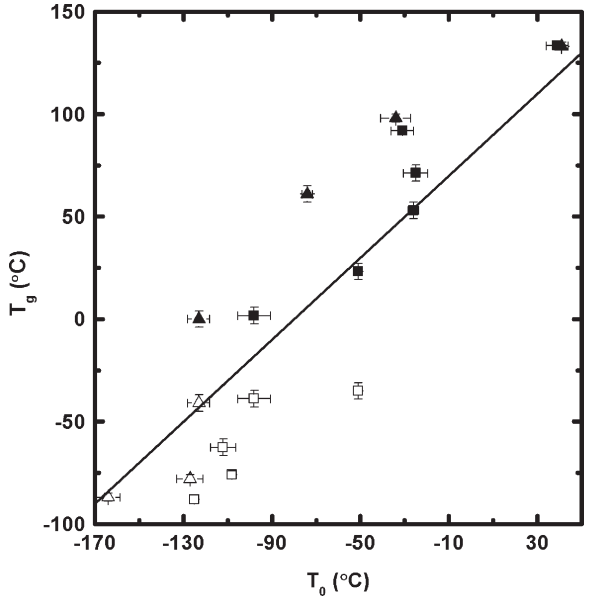

Figure 6. Variation of T_g with T_0 for 125K (squares) and 335K (triangles) PMMA prepared at different weight fractions in [EMI][TFSI]. Open symbols denote T_g data corresponding to ionic liquid T_g peaks, and closed symbols denote T_g data corresponding to PMMA T_g peaks. Solid line represents $T_g = T_0 + 80$ °C.

PMMA concentrations as the T_gs of the systems near 150 °C. Superposition of data from 125K and 335K PMMA shows that there is no dependence of a_T on molecular weight. The fitted values for C_1 and C_2 at T_{ref} = 150 °C are listed in Table 3. With increasing PMMA composition, C_1 increases in value while C_2 decreases in value; these observations are consistent with expectation.[74]

The Vogel temperatures (T_0) of the Vogel−Fulcher−Tammann (VFT) relation have also been estimated for each composition, using the substitution described by Ferry[74] ($T_0 = T_{ref} - C_2$), and are listed in Table 3. With increasing PMMA composition, an increase in T_0 is seen. The values found for pure PMMA (39 °C for 125K PMMA and 41 °C for 335K PMMA) are consistent with the value of T_0 = 35 °C found in the literature.[74] Also, the value of $T_0 = -112$ °C for 30 wt % PMMA ($T_g = -63$ °C) is comparable to the literature value of $T_0 = -128$ °C for a 30% PMMA in the diethyl phthalate system with $T_g = -62$ °C.[74]

In order to compare the results found using DSC against the fitting parameters found using rheometry, T_g values are plotted as a function of T_0 values in Figure 6. For intermediate blend concentrations where two T_g values were extracted by DSC, both values of T_g are included. We anticipate an approximately linear relationship between these values since, generally, $T_g \approx T_0 + 50$ °C. What we

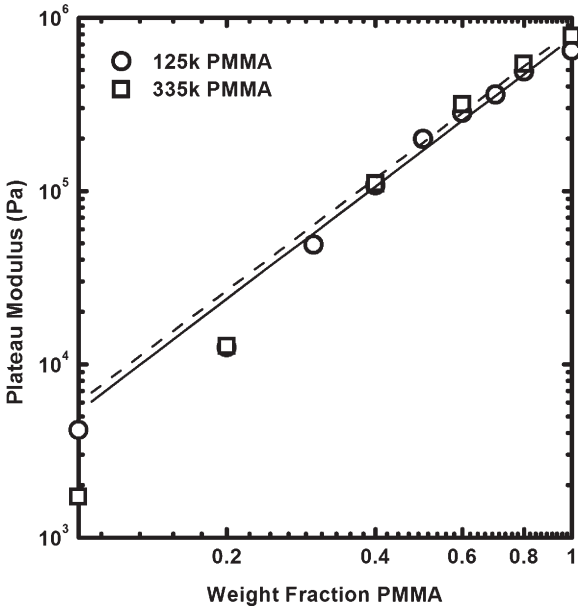

Figure 7. Variation of plateau modulus (G_N) with weight fraction of polymer in [EMI][TFSI] for 125K and 335K PMMA. Lines indicate power law fits to data with PMMA weight fraction >0.2.

observe in the plot is a scattered linear relation; the scatter likely arises from there not being a single representative value for T_g but rather values representing distributions in temperature. The value of T_g exceeds that of T_0 over the whole composition range, but by an amount greater than 50 °C in almost all cases. Such a result has previously been observed for pure PMMA ($T_g - T_0 \approx 80$ °C).[74]

Next, various viscoelastic properties of the PMMA/ionic liquid system are extracted and examined as a function of PMMA composition. The first property of focus is the plateau modulus (G_N), which characterizes the rubbery behavior of the plateau region between the glassy region and terminal region. Since G' in the plateau region cannot be strictly horizontal, various methods have been developed to define G_N.[69,86] In this study, G_N was determined as the value of G' at the frequency where the corresponding curve of tan(δ) exhibits a minimum. These are plotted as a function of PMMA weight fraction on a double-logarithmic scale in Figure 7. The undiluted polymer gives $G_N = 6.5 \times 10^5$ and 8.0×10^5 Pa for 125K and 335K PMMA, respectively; these are slightly higher than the values of $G_N = 4.7 \times 10^5 - 6.2 \times 10^5$ Pa reported in the literature.[63,64] These discrepancies may arise, at least in part, from the different means of defining plateau modulus. Power law fits from the two different molecular weights are the same within error with a slope of 2.2 ± 0.1. (While the technique we employ allows us to define G_N values for even the lowest concentrations without clear plateaus regions, i.e., weight fractions below 20 wt %, these values do not represent the rubbery moduli of an entangled system and are not included in the fits. It can be seen that the data points corresponding to compositions below 20 wt % PMMA lie below the fit lines.) The absence of molecular weight dependence is expected since the plateau modulus is determined by the molecular weight between entanglements. Meanwhile, the power law dependence is close to the value of 2.3 predicted for entangled solutions of neutral polymers in good solvent systems.[72,78,79] Experimental studies of polymer solutions have reported values ranging between 2 and 2.5,[69] and a previous study of PMMA in concentrated diethyl phthalate solutions had found a polymer weight fraction dependence of 2.[63]

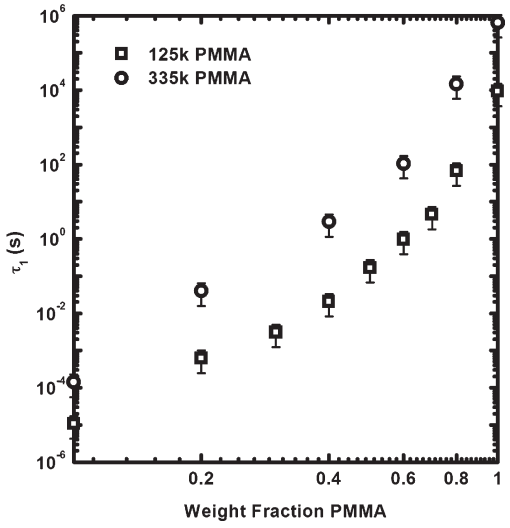

Figure 8. Variation of longest relaxation time (τ_1) at T_{ref} = 150 °C with weight fraction of polymer in [EMI][TFSI] for 125K and 335K PMMA.

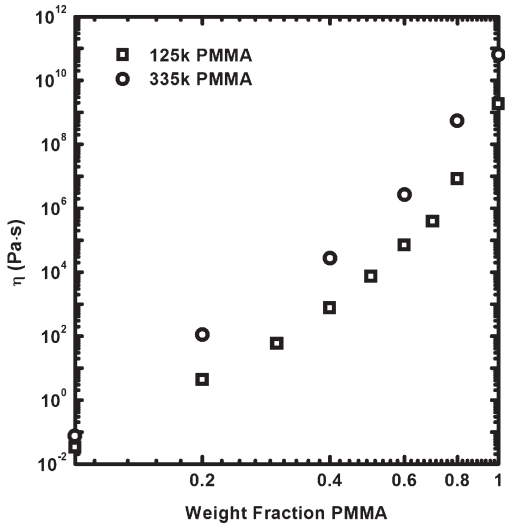

Figure 9. Variation of zero shear viscosity (η) at T_{ref} = 150 °C with weight fraction of polymer in [EMI][TFSI] for 125K and 335K PMMA.

The next property under consideration is the longest relaxation time (τ_1), which defines the time scale required for the system to enter terminal relaxation behavior. Here, this is determined from the value of frequency at the intersection point of lines with slopes 1 and 2 drawn to the terminal regions of G'' and G', respectively. The extracted values of τ_1 are plotted as a function of PMMA composition at a reference temperature of 150 °C in Figure 8 on a log−log scale. An exponential-like increase in τ_1 is seen over 10 decades of time with an increase in PMMA content from 10 to 100 wt %. This reflects the ~2 decade shift in frequency per 20 wt % increase in PMMA composition noted in the discussion of the terminal crossover in the G' and G'' master curves. From Figure 8, we can see the increase from 10 to 20 wt % is noticeably more significant; this can be explained by a shift from the longest relaxation time reflecting unentangled dynamics to one incorporating entanglement. In terms of molecular weight effects, the increase in molecular weight from 125K to 335K yields an increase of ~2 decades in τ_1. The typical power law experimentally reported for reptation time scales (τ_{rep}) as a function of molecular weight (M) is $\tau_{rep} \sim M^{3.5}$.[73] To extract the approximate power law dependence in our system, the data are replotted as τ_1/M^x; a value of $x = 4.5$ is found to give good superposition of the entangled data by eye (Supporting Information Figure S4a). This is higher than the predicted dependence but consistent with higher dependences previously found for PMMA.[87]

Finally, we examine the change in zero shear viscosity (η) with respect to PMMA concentration. We obtain η as $G''(\omega)/\omega$ at low frequencies, and these values are plotted in Figure 9 as a function of PMMA weight fraction at a reference temperature of 150 °C. The graph exhibits an exponential-like dependence on PMMA content, with η exhibiting a much stronger dependence at higher PMMA weight fractions. This change likely reflects effects from shifting from an unentangled to entangled regime as well as from the dramatic change in glass transition over this range of compositions.[63,68,70] There is also a molecular weight effect, as the η values for the 335K samples at a given concentration are 1−2 decades greater than those of the 125K samples. The expected power law dependence for entangled systems is $\eta \sim M^{3.4}$.[73,74] By replotting the data as η/M^x, we find that $x = 3.5$ gives good superposition of the data by eye (see Supporting Information Figure S4b); within error, this is consistent with the expected value.

Scaling laws for concentration (c) dependence have been predicted and studied for τ_1 and η in polymer solutions. However, these are applicable only at a common friction factor[63,68,70,74] (and by extension, a common fractional free volume) across the systems. Given the wide variation and complexity of glass transition temperatures over our systems of study, this is not the case at the reference temperature of 150 °C. As such, the increases in both τ_1 and η found in Figures 8 and 9 are much greater than those predicted by scaling theory (e.g., the basic reptation model predicts $\tau_1 \sim c^{1.6}$ and $\eta \sim c^{3.9}$ for entangled polymer solutions in good solvents).[72] An approximate means of accounting for this is to calculate τ_1 and η values at a constant temperature shift from a characteristic temperature.[88] In Supporting Information Figure S5, we attempt this by recalculating τ_1 and η at a reference temperature of T_0 + 200 K where we apply the T_0 values discussed above from the WLF fits (Tables 3).[63] The results in both cases are highly scattered with a very general trend of increasing τ_1 and η with respect to PMMA weight fraction over a compressed range of τ_1 and η compared with Figures 8 and 9. Treatments based on calculations of fractional free volume as in ref 63 also yielded scattered data.

Conclusions

We have used DSC and rheometry to characterize the glass transition behavior and viscoelastic properties of PMMA/[EMI][TFSI] solutions over the full range of compositions ranging from dilute polymer to pure polymer. The DSC results showed distinct composition dependences for the polymer and ionic liquid components, with two apparent glass transitions at intermediate compositions. The breadths of the glass transitions were much larger for components in the mixtures than for each of the pure components. These results were consistent with expectations of distinct effective local compositions arising from the chain connectivity of the polymer component, as predicted by the Lodge−McLeish model. Rheometry results showed an evolution from unentangled to entangled behavior with increasing concentration as a rubbery plateau region emerged. Accompanying this, moduli also increased, and the transitions between glassy to rubbery and rubbery to terminal behaviors shifted to lower frequencies for samples compared at a common reference temperature. Analyses of the plateau modulus, longest relaxation time, and viscosity showed the general trends expected for solutions of increasing

polymer concentration. The application of time−temperature superposition was successful over the full range of compositions, attesting to the advantages of using nonvolatile ionic liquids as model solvents for viscoelasticity studies.

Acknowledgment. This work was supported by the National Science Foundation through Award DMR-0804197 and by the NSF-REU program in Chemistry at the University of Minnesota (X.L.). Part of this work was carried out in the College of Science & Engineering Polymer Characterization Facility, which has received capital equipment funding from the NSF through the MRSEC (DMR-0212302 and DMR-0819885). We thank Dr. David Giles, Ameara Mansour, and Sangwoo Lee for their assistance with DSC and rheometry experiments.

Supporting Information Available: Figures showing DSC results for 335K PMMA solutions, tTS curves for remaining 125K PMMA solutions, and rescaled τ_1 and η data. This material is available free of charge via the Internet at http://pubs.acs.org.

References and Notes

(1) Lodge, T. P. *Science* **2008**, *321*, 50–51.
(2) Ueki, T.; Watanabe, M. *Macromolecules* **2008**, *41*, 3739–3749.
(3) Lu, J. M.; Yan, F.; Texter, J. *Prog. Polym. Sci.* **2009**, *34*, 431–448.
(4) Scott, M. P.; Brazel, C. S.; Benton, M. G.; Mays, J. W.; Holbrey, J. D.; Rogers, R. D. *Chem. Commun.* **2002**, 1370–1371.
(5) Scott, M. P.; Benton, M. G.; Rahman, M.; Brazel, C. S. *ACS Symp. Ser.* **2003**, *856*, 468–477.
(6) Scott, M. P.; Rahman, M.; Brazel, C. S. *Eur. Polym. J.* **2003**, *39*, 1947–1953.
(7) Rahman, M.; Brazel, C. S. *Polym. Degrad. Stab.* **2006**, *91*, 3371–3382.
(8) Zhang, P. Y.; Peng, L. C.; Li, W. B. *e-Polym.* **2008**, 172.
(9) Katano, H.; Tsukatani, T. *Bull. Chem. Soc. Jpn.* **2010**, *83*, 190–194.
(10) Lunstroot, K.; Driesen, K.; Nockemann, P.; Viau, L.; Mutin, P. H.; Vioux, A.; Binnemans, K. *Phys. Chem. Chem. Phys.* **2010**, *12*, 1879–1885.
(11) Fuller, J.; Breda, A. C.; Carlin, R. T. *J. Electrochem. Soc.* **1997**, *144*, L67–L70.
(12) Carlin, R. T.; Fuller, J. *Chem. Commun.* **1997**, 1345–1346.
(13) Fuller, J.; Breda, A. C.; Carlin, R. T. *J. Electroanal. Chem.* **1998**, *459*, 29–34.
(14) Bansal, D.; Cassel, F.; Croce, F.; Hendrickson, M.; Plichta, E.; Salomon, M. *J. Phys. Chem. B* **2005**, *109*, 4492–4496.
(15) Susan, M. A.; Kaneko, T.; Noda, A.; Watanabe, M. *J. Am. Chem. Soc.* **2005**, *127*, 4976–4983.
(16) Seki, S.; Susan, A. B. H.; Kaneko, T.; Tokuda, H.; Noda, A.; Watanabe, M. *J. Phys. Chem. B* **2005**, *109*, 3886–3892.
(17) Li, Z. H.; Jiang, J.; Lei, G. T.; Gao, D. S. *Polym. Adv. Technol.* **2006**, *17*, 604–607.
(18) Shobukawa, H.; Tokuda, H.; Susan, M. A. H.; Watanabe, M. *Electrochim. Acta* **2005**, *50*, 3872–3877.
(19) Brown, R. H.; Duncan, A. J.; Choi, J. H.; Park, J. K.; Wu, T. Y.; Leo, D. J.; Winey, K. I.; Moore, R. B.; Long, T. E. *Macromolecules* **2010**, *43*, 790–796.
(20) He, Y. Y.; Boswell, P. G.; Buhlmann, P.; Lodge, T. P. *J. Phys. Chem. B* **2007**, *111*, 4645–4652.
(21) He, Y. Y.; Lodge, T. P. *Chem. Commun.* **2007**, 2732–2734.
(22) He, Y.; Lodge, T. P. *Macromolecules* **2008**, *41*, 167–174.
(23) Noro, A.; Matsushita, Y.; Lodge, T. P. *Macromolecules* **2009**, *42*, 5802–5810.
(24) Virgili, J. M.; Hexemer, A.; Pople, J. A.; Balsara, N. P.; Segalman, R. A. *Macromolecules* **2009**, *42*, 4604–4613.
(25) Virgili, J. M.; Nedoma, A. J.; Segalman, R. A.; Balsara, N. P. *Macromolecules* **2010**, *43*, 3750–3756.
(26) Virgili, J. M.; Hoarfrost, M. L.; Segalman, R. A. *Macromolecules* **2010**, *43*, 5417–5423.
(27) Simone, P. M.; Lodge, T. P. *Macromolecules* **2008**, *41*, 1753–1759.
(28) Simone, P. M.; Lodge, T. P. *ACS Appl. Mater. Interfaces* **2009**, *1*, 2812–2820.
(29) Lee, J.; Panzer, M. J.; He, Y. Y.; Lodge, T. P.; Frisbie, C. D. *J. Am. Chem. Soc.* **2007**, *129*, 4532–4533.
(30) Cho, J. H.; Lee, J.; Xia, Y.; Kim, B.; He, Y. Y.; Renn, M. J.; Lodge, T. P.; Frisbie, C. D. *Nature Mater.* **2008**, *7*, 900–906.
(31) Cho, J. H.; Lee, J.; He, Y.; Kim, B.; Lodge, T. P.; Frisbie, C. D. *Adv. Mater.* **2008**, *20*, 686–690.
(32) Lee, J.; Kaake, L. G.; Cho, J. H.; Zhu, X. Y.; Lodge, T. P.; Frisbie, C. D. *J. Phys. Chem. C* **2009**, *113*, 8972–8981.
(33) Gwee, L.; Choi, J. H.; Winey, K. I.; Elabd, Y. A. *Polymer* **2010**, *51*, 5516–5524.
(34) Rodriguez, H.; Rogers, R. D. *Fluid Phase Equilib.* **2010**, *294*, 7–14.
(35) He, Y. Y.; Li, Z. B.; Simone, P.; Lodge, T. P. *J. Am. Chem. Soc.* **2006**, *128*, 2745–2750.
(36) Simone, P. M.; Lodge, T. P. *Macromol. Chem. Phys.* **2007**, *208*, 339–348.
(37) Ueki, T.; Watanabe, M.; Lodge, T. P. *Macromolecules* **2009**, *42*, 1315–1320.
(38) Tamura, S.; Ueki, T.; Ueno, K.; Kodama, K.; Watanabe, M. *Macromolecules* **2009**, *42*, 6239–6244.
(39) Meli, L.; Lodge, T. P. *Macromolecules* **2009**, *42*, 580–583.
(40) Meli, L.; Santiago, J. M.; Lodge, T. P. *Macromolecules* **2010**, *43*, 2018–2027.
(41) Bai, Z. F.; Lodge, T. P. *J. Phys. Chem. B* **2009**, *113*, 14151–14157.
(42) Bai, Z. F.; Lodge, T. P. *Langmuir* **2010**, *26*, 8887–8892.
(43) Anderson, J. L.; Ding, J.; Welton, T.; Armstrong, D. W. *J. Am. Chem. Soc.* **2002**, *124*, 14247–14254.
(44) Fox, T. G. *Bull. Am. Phys. Soc.* **1956**, *1*, 123.
(45) Gordon, M.; Taylor, J. S. *J. Appl. Chem.* **1952**, *2*, 493.
(46) Braun, G.; Kovacs, A. J. *Phys. Non-Cryst Solids Proc. Int. Conf.* **1965**, *1964*, 303–318.
(47) Hains, P. J.; Williams, G. *Polymer* **1975**, *16*, 725–729.
(48) Scandola, M.; Ceccorulli, G.; Pizzoli, M.; Pezzin, G. *Polym. Bull.* **1982**, *6*, 653–660.
(49) Pizzoli, M.; Scandola, M.; Ceccorulli, G.; Pezzin, G. *Polym. Bull.* **1983**, *9*, 429–436.
(50) Ceccorulli, G.; Pizzoli, M.; Scandola, M. *Polymer* **1987**, *28*, 2077–2080.
(51) Scandola, M.; Ceccorulli, G.; Pizzoli, M. *Polymer* **1987**, *28*, 2081–2084.
(52) Righetti, M. C.; Ajroldi, G.; Pezzin, G. *Polymer* **1992**, *33*, 4779–4785.
(53) Righetti, M. C.; Ajroldi, G.; Pezzin, G. *Polymer* **1992**, *33*, 4786–4792.
(54) Savin, D. A.; Larson, A. M.; Lodge, T. P. *J. Polym. Sci., Part B: Polym. Phys.* **2004**, *42*, 1155–1163.
(55) Taniguchi, N.; Urakawa, O.; Adachi, K. *Macromolecules* **2004**, *37*, 7832–7838.
(56) Lutz, T. R.; He, Y. Y.; Ediger, M. D. *Macromolecules* **2005**, *38*, 9826–9835.
(57) Ediger, M. D.; Lutz, T. R.; He, Y. Y. *J. Non-Cryst. Solids* **2006**, *352*, 4718–4723.
(58) Lipson, J. E. G.; Milner, S. T. *J. Polym. Sci., Part B: Polym. Phys.* **2006**, *44*, 3528–3545.
(59) Cangialosi, D.; Alegria, A.; Colmenero, J. *J. Chem. Phys.* **2007**, *126*, 204904.
(60) Lodge, T. P.; McLeish, T. C. B. *Macromolecules* **2000**, *33*, 5278–5284.
(61) Lodge, T. P.; Wood, E. R.; Haley, J. C. *J. Polym. Sci.; Part B: Polym. Phys.* **2006**, *44*, 756–763.
(62) Gaikwad, A. N.; Wood, E. R.; Ngai, T.; Lodge, T. P. *Macromolecules* **2008**, *41*, 2502–2508.
(63) Masuda, T.; Toda, N.; Aoto, Y.; Onogi, S. *Polym. J.* **1972**, *3*, 315–321.
(64) Graessley, W. W.; Edwards, S. F. *Polymer* **1981**, *22*, 1329–1334.
(65) Takahashi, Y.; Noda, I.; Nagasawa, M. *Macromolecules* **1985**, *18*, 2220–2225.
(66) Osaki, K.; Nishimura, Y.; Kurata, M. *Macromolecules* **1985**, *18*, 1153–1157.
(67) Colby, R. H.; Rubinstein, M. *Macromolecules* **1990**, *23*, 2753–2757.
(68) Colby, R. H.; Fetters, L. J.; Funk, W. G.; Graessley, W. W. *Macromolecules* **1991**, *24*, 3873–3882.
(69) Tao, H.; Huang, C.; Lodge, T. P. *Macromolecules* **1999**, *32*, 1212–1217.
(70) Tao, H.; Lodge, T. P.; von Meerwall, E. D. *Macromolecules* **2000**, *33*, 1747–1758.
(71) Heo, Y.; Larson, R. G. *Macromolecules* **2008**, *41*, 8903–8915.
(72) Colby, R. H. *Rheol. Acta* **2010**, *49*, 425–442.
(73) Rubinstein, M.; Colby, R. H. In *Polymer Physics*; Oxford University Press: New York, 2003.
(74) Ferry, J. D. In *Viscoelastic Properties of Polymers*, 3rd ed.; John Wiley & Sons: New York, 1980.

(75) von Meerwall, E. D.; Amelar, S.; Smeltzly, M. A.; Lodge, T. P. *Macromolecules* **1989**, *22*, 295–304.
(76) Rizos, A.; Fytas, G.; Lodge, T. P.; Ngai, K. L. *J. Phys. Chem.* **1991**, *95*, 2980–2987.
(77) Santangelo, P. G.; Ngai, K. L.; Roland, C. M. *Macromolecules* **1994**, *27*, 3859–3863.
(78) Ueno, K.; Inaba, A.; Kondoh, M.; Watanabe, M. *Langmuir* **2008**, *24*, 5253–5259.
(79) The ionic liquid [EMI][TFSI] is considered to be a good solvent for PMMA,[78] and the two have been found to be compatible over all compositions studied.[15,16] However, the χ parameter calculated for this system is >0.5.[78] These results were contrary to the observed experimental results,[78] and it was concluded that the calculation of χ from solubility parameters was not a reliable predictor of solubility.
(80) Zeroni, I.; Ozair, S.; Lodge, T. P. *Macromolecules* **2008**, *41*, 5033–5041.
(81) Mok, M. M.; Kim, J.; Wong, C. L. H.; Marrou, S. R.; Woo, D. J.; Dettmer, C. M.; Nguyen, S. T.; Ellison, C. J.; Shull, K. R.; Torkelson, J. M. *Macromolecules* **2009**, *42*, 7863–7876.
(82) Kumar, S. K.; Shenogin, S.; Colby, R. H. *Macromolecules* **2007**, *40*, 5759–5766.
(83) Shenogin, S.; Kant, R.; Colby, R. H.; Kumar, S. K. *Macromolecules* **2007**, *40*, 5767–5775.
(84) Hiemenz, P. C.; Lodge, T. P. In *Polymer Chemistry*, 2nd ed.; Taylor & Francis Group: Tampa, FL, 2007.
(85) Ngai, K. L.; Plazek, D. J. *Rubber Chem. Technol.* **1995**, *68*, 376–434.
(86) Graessley, W. W. *Adv. Polym. Sci.* **1974**, *16*, 1–179.
(87) Osaki, K.; Takatori, E.; Watanabe, H.; Kotaka, T. *Rheol. Acta* **1993**, *32*, 132–139.
(88) Marchionni, G.; Ajroldi, G.; Pezzin, G. *Eur. Polym. J.* **1988**, *24*, 1211–1216.